

## Splitting Schemes for the Numerical Solution of a Two-Dimensional Vlasov Equation

MAGDI M. SHOUCRI AND REAL R. J. GAGNÉ

*Department of Electrical Engineering, Laval University, Quebec, Canada*

Received July, 1976; revised May 4, 1977

Splitting schemes are applied to the numerical solution of a two-dimensional Vlasov equation. Results obtained when solving the equation in configuration space, by treating the convective term and the acceleration term separately, are compared with results previously obtained using a different method where the two-dimensional Vlasov equation was transformed in velocity space using Hermite polynomials expansion.

### 1. INTRODUCTION

Splitting schemes have been successfully applied to the solution of the Vlasov equation [1-3]. For the one-dimensional case [1], the Vlasov equation was integrated in the original phase space by applying a method of fractional steps [4], which consisted of treating the convective term and the acceleration term separately; these terms were computed at each time step using Fourier interpolation and spline interpolation methods, respectively, and the overall scheme was of second order in  $\Delta t$ . The results obtained by this method are very accurate and efficient and can be readily extended to higher dimensions. It is the purpose of the present work to extend this method to two dimensions. The results obtained by this method will be compared to the results previously reported [2] for the numerical solution of the two-dimensional Vlasov equation, where the distribution function was first expanded in velocity space using a Hermite polynomials expansion, and the resulting equation integrated alternatively in the  $x$  and  $y$  directions.

In Section 2, we indicate how the method reported in [1] can be extended to two dimensions. In Section 3 we present the numerical results obtained for the free streaming case, the linear Landau damping, and the nonlinear equation. These results are then compared with those recently reported in [2], using the Hermite polynomials expansion. Section 4 presents the conclusions.

### 2. THE SPLITTING SCHEME

The generalization of the splitting scheme derived by Cheng and Knorr [1] to two dimensions is straightforward; we only have to use the vectorial notation  $\mathbf{v}$  and  $\mathbf{r}$

for the velocity and the position, and the derivation of the second-order scheme is identical [1]. In order to fix the notation, we indicate here the important steps in this derivation. We want to solve the dimensionless system:

$$\frac{\partial f}{\partial t}(\mathbf{r}, \mathbf{v}, t) + \mathbf{v} \cdot \frac{\partial f}{\partial \mathbf{r}}(\mathbf{r}, \mathbf{v}, t) + \mathbf{E}(\mathbf{r}, \mathbf{v}, t) \cdot \frac{\partial f}{\partial \mathbf{v}}(\mathbf{r}, \mathbf{v}, t) = 0, \quad (1a)$$

$$\nabla \cdot \mathbf{E} = \int_{-\infty}^{\infty} f(\mathbf{r}, \mathbf{v}, t) d\mathbf{v} - 1 \quad (1b)$$

for periodic boundary conditions in  $\mathbf{r}$  (the different symbols have their conventional meaning). We split Eq. (1a) and solve, for the first half time-step, the free streaming term.

$$\frac{\partial f}{\partial t} + \mathbf{v} \cdot \frac{\partial f}{\partial \mathbf{r}} = 0, \quad (2)$$

and for the second half time-step we solve the acceleration term:

$$\frac{\partial f}{\partial t} + \mathbf{E}(\mathbf{r}, t) \cdot \frac{\partial f}{\partial \mathbf{v}} = 0. \quad (3)$$

A formal implicit solution of Eqs. (2)–(3) is given by the following sequence of shifts of the distribution function [1]:

$$f^*(\mathbf{r}, \mathbf{v}) = f^n(\mathbf{r} - \mathbf{v} \Delta t/2, \mathbf{v}), \quad (4)$$

$$f^{**}(\mathbf{r}, \mathbf{v}) = f^*(\mathbf{r}, \mathbf{v} - \mathbf{E}(\mathbf{r}) \Delta t) \quad (5)$$

$$f^{n+1}(\mathbf{r}, \mathbf{v}) = f^{**}(\mathbf{r} - \mathbf{v} \Delta t/2, \mathbf{v}), \quad (6)$$

where  $\Delta t$  is the time-step, and the superscript  $n$  denotes that the quantity is calculated at a time-step  $t = n \Delta t$ . The electric field in Eq. (5) is calculated from  $f^*(\mathbf{r}, \mathbf{v})$  of Eq. (4) and used in Eq. (5) to operate the shift. The formal solution given in Eqs. (4)–(6) is equivalent to a second-order scheme in  $\Delta t$  [1]. We note that the successive shifts can be started in either  $x$  or  $y$  for Eqs. (4) and (6), and in either  $v_x$  or  $v_y$  for Eq. (5).

The solution of the Vlasov equation has thus been reduced to the interpolation problems given in Eqs. (4)–(6). A study of the interpolation of  $f$  in the  $\mathbf{r}$  and  $\mathbf{v}$  directions has been given for the one-dimensional case in [1]. The generalization to two dimensions is straightforward. In [1], a Fourier interpolation scheme was used for Eq. (4); this, however, requires an execution time proportional to  $N^2$  (where  $N$  is the number of points), which increases the computational effort when a large number of points is used, or when working with dimensions higher than one. In order to minimize the computational effort we use, in our case, a cubic spline interpolation [4] where the number of operations grows with  $N$  only. Whether  $f$  in Eq. (4) is interpolated in the  $x$  direction or in the  $y$  direction first is immaterial. The interpolated values  $f^*(\mathbf{r}, \mathbf{v})$  are then used to calculate the electric field  $\mathbf{E}(\mathbf{r}, t)$ , used in Eq. (5) for the shift. This is

started in either the  $v_x$  direction or the  $v_y$  direction. A cubic spline interpolation is once more used to calculate  $f^{**}(\mathbf{r}, \mathbf{v})$ ; the distribution function is finally shifted, as in Eq. (6), to obtain  $f^{n+1}(\mathbf{r}, \mathbf{v}, t)$ . It should be noted that periodic boundary conditions are used in space, while the distribution function  $f$  is assumed to be zero for  $|\mathbf{v}| > V_{\max}$ .

### 3. NUMERICAL RESULTS

A rectangular mesh will be used to represent the  $\mathbf{r}$ - $\mathbf{v}$  phase space with the computational domain

$$R = \{(\mathbf{r}, \mathbf{v}) \mid 0 \leq x \leq L_x, 0 \leq y \leq L_y, |v_x| \leq V_{x \max}, |v_y| \leq V_{y \max}\};$$

where  $L_x$  and  $L_y$  are the spatial periodic lengths in the  $x$  and  $y$  directions, respectively,  $V_{x \max}$  and  $V_{y \max}$  are the cutoff velocities for  $v_x$  and  $v_y$ , while  $N_x$ ,  $N_y$ ,  $2M_x$ , and  $2M_y$  designate the numbers of mesh points used along the directions  $x$ ,  $y$ ,  $v_x$ , and  $v_y$ , respectively.

The numerical results described below are intended to demonstrate the accuracy, the efficiency, and the stability of the two-dimensional splitting scheme; comparison with the previously reported results using Hermite polynomials expansion [2] will be made to demonstrate the economy of the present scheme in terms of computational effort.

The first example shows the recurrence effect of the free streaming equation, when the electric field in Eq. (1a) is neglected, i.e., when solving Eq. (2) alone. The results in Fig. 1 have been obtained by plotting on a logarithmic scale the absolute value of the density

$$\rho(\mathbf{r}, t) = \int_{-\infty}^{\infty} f(\mathbf{r}, \mathbf{v}, t) d\mathbf{v} \quad (7)$$

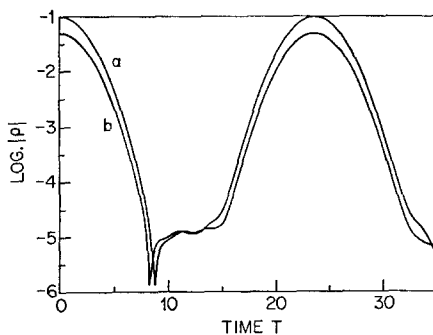


FIG. 1. Time evolution of the density  $\rho(\mathbf{r}, t)$  at positions  $x = 0, y = 0$  (curve  $\bar{a}$ ) and  $x = L_x/4, y = 0$  (curve  $\bar{b}$ ), for the free streaming case, and for the initial conditions in Eq. (8).

at the respective positions  $x = 0, y = 0$  (curve a), and  $x = L_x/4, y = 0$  (curve b). The initial value of the distribution function is given by:

$$f(\mathbf{r}, \mathbf{v}, 0) = f_0(\mathbf{v})(A_x \cos k_x x + A_y \cos k_y y), \quad (8)$$

with  $A_x = A_y = 0.05, L_x = L_y = 4\pi$ , hence  $k_x = k_y = k = 0.5$  and

$$f_0(\mathbf{v}) = (1/2\pi) e^{-\frac{1}{2}v_x^2 - \frac{1}{2}v_y^2}. \quad (9)$$

The solution of Eq. (2) is given by:

$$f(\mathbf{r}, \mathbf{v}, t) = f(\mathbf{r} - \mathbf{v}t, \mathbf{v}, 0). \quad (10)$$

Equation (10), combined with Eqs. (7) and (8), leads to the following expression for the density:

$$\rho(\mathbf{r}, t) = e^{-k^2 t^2/2}(A_x \cos k_x x + A_y \cos k_y y). \quad (11)$$

Numerical calculation of Eq. (7), on the other hand, gives the following expression for the density

$$\begin{aligned} \rho(\mathbf{r}, t) &= \sum_{i=-M_x}^{M_x-1} \sum_{j=-M_y}^{M_y-1} f(x - v_{x_i} t, y - v_{y_j} t, 0) \Delta v_x \Delta v_y, \quad (12) \\ &= \Delta v_x \Delta v_y \sum_{i=-M_x}^{M_x-1} \sum_{j=-M_y}^{M_y-1} f_0(v_{x_i}, v_{y_j})(A_x \cos(k_x x - (i + \frac{1}{2}) k_x \Delta v_x t) \\ &\quad + A_y \cos(k_y y - (j + \frac{1}{2}) k_y \Delta v_y t)). \quad (13) \end{aligned}$$

The right-hand side of Eq. (13) is the sum of periodic functions of time which results in a quasi-periodic behavior for  $\rho(\mathbf{r}, t)$  instead of the exponential decay given in Eq. (11). In the present calculation  $k_x = k_y = 0.5, V_{x \max} = V_{y \max} = 4$ , and  $M_x = M_y = 8$ . The early parts of the curves in Fig. (1) show the exponential decay in time, as predicted by Eq. (11), followed by the recurrence effect; for a square matrix, like that in the present case, the predicted recurrence time is  $T_R = 2\pi/(k \Delta v) = 23.56$ , and the numerical results presented in Fig. 1 agree very well with this value. The calculations were done using a value of  $\Delta t = 1/8$ . If, instead of Eq. (8), we use the following initial condition

$$f(\mathbf{r}, \mathbf{v}, 0) = f_0(\mathbf{v})(1 + A_x \cos kx + A_y \cos ky) \quad (14)$$

(where  $f_0(\mathbf{v})$  is given in Eq. (9)), we get, instead of Eq. (11), the following expression for the density

$$\rho(\mathbf{r}, t) = 1 + e^{-k^2 t^2/2}(A_x \cos kx + A_y \cos ky). \quad (15)$$

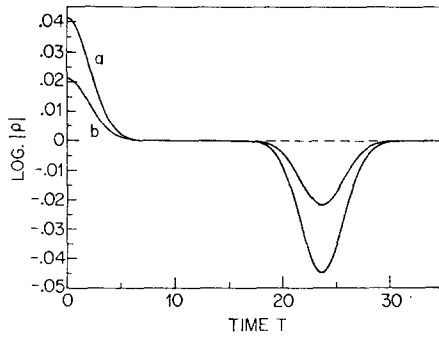


FIG. 2. Time evolution of the density  $\rho(\mathbf{r}, t)$  at positions  $x = 0, y = 0$  (curve a) and  $x = L_x/4, y = 0$  (curve b), for the free streaming case, and for the initial conditions in Eq. (14).

Numerical calculation, however, gives the same expression for the density as in Eq. (12), provided  $\rho(\mathbf{r}, t)$ , in the right-hand side of this equation, is replaced by  $(\rho(\mathbf{r}, t) - 1)$ . The results in this case are shown in Fig. 2, where the absolute values of  $\rho(\mathbf{r}, t)$  are plotted on a logarithmic scale against time, for the positions  $x = 0, y = 0$  (curve a), and  $x = L_x/4, y = 0$  (curve b). The parameters are the same as in Fig. 1. As can be verified from Eq. (15),  $\log |\rho| \rightarrow 0$  as  $t \rightarrow \infty$ , and the curves in Fig. 2 tend asymptotically to 0, in agreement with Eq. (15). A recurrence effect occurs at a recurrence time  $T_R = 23.56$ .

The full curve presented in Fig. 3 has been obtained for the linear Landau damping, by solving the linearized form of Eq. (1). The initial condition was, for the linearized part of the distribution function

$$f(\mathbf{r}, \mathbf{v}, 0) = A_x f_0(\mathbf{v}) \cos k_x x \cos k_y y, \tag{16}$$

with  $A_x = 0.05, k_x = k_y = 0.5$ , and  $f_0(\mathbf{v})$  as given in Eq. (9). While the full curve has been obtained with the scheme of interest here, the dotted curve has been obtained

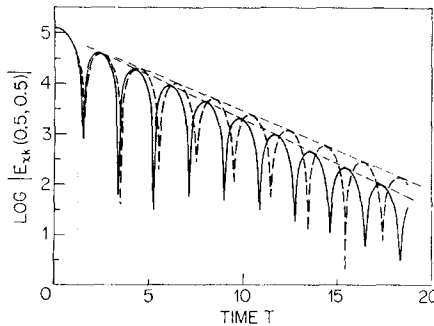


FIG. 3. Numerical solution for the linearized 2D Vlasov equation. Full curve: direct integration in phase space; Dotted curve: the distribution function is first transformed in velocity space using Hermite polynomials expansion.

using the Hermite polynomials expansion of the distribution function [2], and is given here for reference. With both methods the Fourier mode  $E_{xk}(0.5, 0.5)$  of the  $x$  component of the electric field  $E_x$  and the Fourier mode  $E_{yk}(0.5, 0.5)$  of the  $y$  components of the electric field  $E_y$  are present, at  $t = 0$ , and decay exponentially in time while remaining exactly equal to each other. The dotted curve has been obtained with a mesh of  $8 \times 8$  points and  $40 \times 40$  polynomials, and necessitated a computational time (CPU time) of about 250 min using an IBM 370/155; a time-step  $\Delta t = 1/16$  was used because the code was found to be numerically unstable for larger values of  $\Delta t$ . The full curve was calculated using the same initial conditions (Eq. (16)) that were used for the dotted curve, and the calculations were carried out up to the same maximum time ( $t = 18.75$ ); meshes of  $8 \times 8$  points in configuration space and  $32 \times 32$  points in velocity space were used, so that the dimensions of the matrices were approximately equal to those previously used in the case of Hermite polynomials expansion. The execution time in this case (CPU time) was about 67 min compared with 250 min for the Hermite polynomials expansion (using the same IBM machine). An important part of the economy in execution time is due to the fact that the calculations were made with a value of  $\Delta t = 1/8$ , without any numerical instability appearing. We note, however, that  $\Delta t$  has been increased only by a factor of 2, while the actual decrease in computation time is by a factor  $250/67 \approx 3.7$ . Furthermore, the present calculations give  $\omega/\omega_p = 1.675$  and  $\gamma/\omega_p = 0.400$  (where  $\omega$  and  $\gamma$  are the real and imaginary parts of the frequency, respectively, and  $\omega_p$  is the plasma frequency), in much closer agreement with the theoretical values ( $\omega/\omega_p = 1.682$ ,  $\gamma/\omega_p = 0.394$ ) than the values obtained using the Hermite polynomials expansion [2] ( $\omega/\omega_p = 1.58$ ,  $\gamma/\omega_p = 0.35$ ).

Finally, Figs. 4-6 show the results obtained when solving the full nonlinear Vlasov equation, using the same initial conditions that were used for Eq. (14). These conditions were also used when solving the full nonlinear equation using a Hermite polynomials expansion with meshes of  $16 \times 16$  points and  $30 \times 30$  polynomials, as reported in [2]. For the present calculations we use a mesh of  $16 \times 16$  points in configuration space and a mesh of  $32 \times 32$  points in velocity space; the dimensions

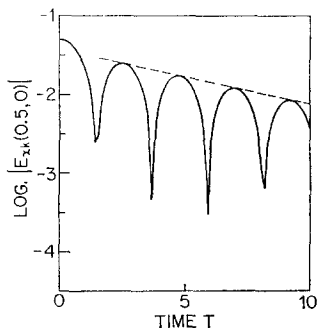


FIG. 4. Plot of the logarithm of the fundamental mode  $|E_{xk}(0.5, 0)|$  for the solution of the nonlinear Vlasov equation, using the initial condition in Eq. (14).

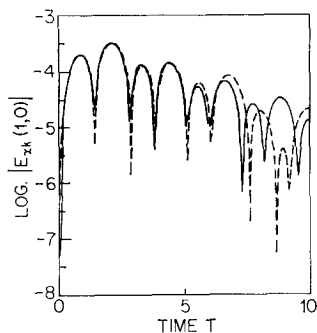


FIG. 5. Plot, on a logarithmic scale, of the magnitude of the mode  $E_{xk}(1, 0)$  which is excited when solving the full nonlinear equation. The dotted curve corresponds to the curve obtained in [2] by expanding the distribution function in velocity space using Hermite polynomials.

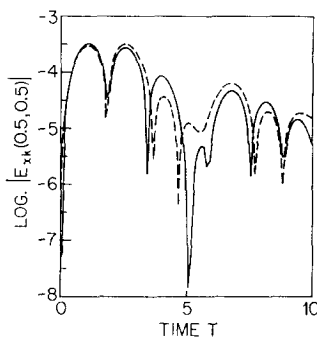


FIG. 6. Plot, on a logarithmic scale, of the magnitude of the mode  $E_{xk}(0.5, 0.5)$  which is excited when solving the full nonlinear equation. The dotted curve corresponds to the curve obtained in [2] by expanding the distribution function in velocity space using Hermite polynomials.

of the matrices are thus approximately equal to those for the Hermite expansion method. It took about 90 min of execution time, with a time-step  $\Delta t = 1/8$ , to pursue the calculations up to  $t = 10.0$ , using an IBM 370/168.

One expects linear Landau damping to dominate at the early evolution of the system, and, in agreement with this, the two modes  $E_{xk}(0.5, 0)$  and  $E_{yk}(0, 0.5)$ , present at  $t = 0$ , were found to decay linearly and to remain exactly equal to each other, up to  $t = 10.0$ . Figure 4 shows the plot of  $|E_{xk}(0.5, 0)|$  on a logarithmic scale. The numerical values of  $\omega/\omega_p$  and  $\gamma/\omega_p$  are 1.42 and 0.154, respectively, which agree fairly well with the theoretical values of 1.415 and 0.1533, respectively. The corresponding results reported in [2], when using the Hermite polynomials expansion, necessitated an execution time of almost 4 hr, using the same IBM machine, with a time-step  $\Delta t = 1/16$  (larger values of  $\Delta t$  resulted in numerical instabilities). The fundamental mode in that case decayed linearly [2], with  $\omega/\omega_p = 1.48$  and  $\gamma/\omega_p = 0.158$ , and, hence, had a behavior almost identical to that observed in Fig. 4.

Figure 5 and 6 show the higher modes  $E_{xk}(1, 0)$ , and  $E_{xk}(0.5, 0.5)$ ; the amplitudes

of these modes are found to remain at least two orders of magnitude smaller than that of the fundamental  $E_{yk}$  mode. Furthermore, these two modes were found to be identical in behavior to the two modes  $E_{yk}(0, 1)$  and  $E_{yk}(0.5, 0.5)$ , respectively. The dotted curves in Figs. 5 and 6 show, for comparison purposes, the results previously obtained using the Hermite polynomials expansion [2]. For the higher modes, as can be seen, small differences exist between the curves obtained by the two techniques discussed.

#### 4. CONCLUSION

In the present work, we have compared the results obtained for the solution of a two-dimensional Vlasov equation, using two different splitting schemes: one in which the equation is integrated in phase space, by treating the convective term and the acceleration term separately, and another, previously reported in [2], where the equation is first transformed in velocity space using Hermite polynomials expansion. The present results show that for the range of parameters used, the method of direct integration in phase space is more accurate and more economical than the method previously reported in [2]. Most of the economy is due to the fact that the presently reported results were calculated with  $\Delta t = 1/8$ , while for the method reported in [2], the calculations were done with  $\Delta t = 1/16$ , since higher values of  $\Delta t$  were accompanied by numerical instabilities. What advantage this method may have in other parts of the parameter space (especially for very small values of the wavenumbers) is still to be investigated; we note, however, that the method has been recently extended to a three-dimensional magnetized plasma [6], with a time-step  $\Delta t$  which can be of the order of 1, which makes it even more advantageous than was reported in [2].

#### ACKNOWLEDGMENTS

The authors are grateful to the staff of the Computer Center of Laval University for much assistance. The authors are also grateful to the "Direction de l'Enseignement Supérieur", for special permission to use the IBM 370/168 of the Ministry of Education of the Provincial Government of Quebec (SIMEQ); they also wish to express their gratitude to the SIMEQ authorities and to Mr. J.-J. Raymond for his constant help. The constant support and encouragement of Mr. M. Lecours, Head of the Electrical Engineering Department, is also gladly acknowledged. Mr. Shoucri is grateful to professor G. Knorr and Dr. C.-Z. Cheng for many discussions.

#### REFERENCES

1. C.-Z. CHENG AND G. KNORR, "The Integration of the Vlasov Equation in Configuration Space," University of Iowa, Rep. No. 75-24 (1975); M. M. SHOUCRI AND R. R. J. GAGNÉ, *J. Computational Physics*, to appear.
2. M. M. SHOUCRI AND R. R. J. GAGNÉ, *J. Computational Phys.* **23** (1977), 242.
3. J. BYERS AND J. KILLEEN, in "Methods in Computational Physics," Vol. 9, p. 259, Academic Press, New York, 1969.
4. N. N. YANENKO, "The Method of Fractional Steps," Springer-Verlag, New York, 1971.
5. F. B. HILDEBRAND, "Introduction to Numerical Analysis," Chap. 9, McGraw-Hill, New York, 1974.
6. C.-Z. CHENG, Princeton Plasma Physics Laboratory Rep. Matt.-1247; *J. Computational Phys.*, to appear.